Computers and Electronics in Agriculture 137 (2017) 138–149

Contents lists available at ScienceDirect

Computers and Electronics in Agriculture

journal homepage: www.elsevier.com/locate/compag

Original papers

An intelligent integrated control of hybrid hot air-infrared dryer based on fuzzy logic and computer vision system

Mohammad Hossein Nadian [a,b], Mohammad Hossein Abbaspour-Fard [a,*], Alex Martynenko [c], Mahmood Reza Golzarian [a]

[a] Department of Biosystems Engineering, Ferdowsi University of Mashhad, Mashhad, Iran
[b] Brain Engineering Research Center, Institute for Research in Fundamental Sciences (IPM), P.O. Box 19395-5531, Tehran, Iran
[c] Department of Engineering, Dalhousie University, Canada

ARTICLE INFO

Article history:
Received 8 February 2016
Received in revised form 13 March 2017
Accepted 3 April 2017

Keywords:
Kiwifruit
Fuzzy control
Genetic algorithm
Hybrid hot air-infrared dryer
Computer vision system

ABSTRACT

In this study, an intelligent fuzzy-machine vision control system (FMCS) was developed to control the operating variables throughout a hybrid hot air-infrared drying process. The total discoloration and the shrinkage of thin layer kiwifruit slices were monitored in real time using a computer vision system (CVS). These values along with calculated energy consumption obtained from preliminary experiments, were fed into a genetic algorithm (GA) framework to optimize a fuzzy logic control system. The performance of the fuzzy controller was evaluated for kiwifruit drying using a laboratory-scale hot air-infrared dryer. The results indicated that the hybrid drying could significantly reduce the drying load/time compared with the hot air drying. The FMCS application showed a good balance between energy consumption (0.158 kW h) and product quality ($\Delta E = 2.32$).

1. Introduction

Preventing unfavorable changes of product quality is a crucial task in food industry. Shrinkage and color are considered the most important organoleptic properties, determining marketability of the product after drying. To avoid unfavorable changes of organoleptic properties, the quality of food must be accurately and rapidly detected using real time computer vision system (CVS). An online CVS can continuously collect information about the shape, size (Campos-Mendiola et al., 2007; Hosseinpour et al., 2011; Yadollahinia and Jahangiri, 2009) and color (Chen and Martynenko, 2013; Hosseinpour et al., 2013; Nadian et al., 2015) of the food product in the process of drying.

Another crucial task in food industry and particularly in drying is to maximize the profitability due to reducing the associated costs. In this regard, reducing energy consumption is the main concern because industrial dryers consume a significant part of the total energy, i.e. 12% on average (Mujumdar, 2014). Generally, the reduction of drying time is a possible avenue to increase the efficiency of operation. Hence, hybrid technologies such as microwave- and infrared-assisted convective drying becoming more popular (Hebbar et al., 2004; Zhang et al., 2006). Although such combined technologies are more efficient than hot-air drying (HAD), the deterioration of organoleptic properties of the end product is of significant concern. The problem is that without careful monitoring the sample temperature may still continue to rise, resulting in overheating or burning (Zhang et al., 2010). Since most foods are heat-sensitive in nature, it is desirable to implement intelligent control system, such as neural networks or fuzzy logic, to preserve product quality.

Fuzzy control systems are applied in nonlinear and probabilistic processes, or for the situations where processes could not be modeled mathematically (Herrera et al., 1998). In addition, the organoleptic characteristics of foods are imprecise attributes with no defined boundaries. However, using linguistic attributes they could be characterized as high, low and medium quality, etc. Considering these inherent characteristics, fuzzy logic control seems to be appropriate approach for foodstuff applications in such as drying (Li et al., 2010). Hence, a fuzzy-machine vision control system (FMCS) application, which combines a CVS to continuously extract visual information of agro-food product under drying and sends this information to a fuzzy control system, can be a suitable alternative to traditional control strategy. Although most of research with CVS has been done in image-based quality monitoring of drying process, to the best of authors' knowledge, no development is

* Corresponding author.
E-mail address: abaspour@um.ac.ir (M.H. Abbaspour-Fard).

http://dx.doi.org/10.1016/j.compag.2017.04.001
0168-1699/

Nomenclature

HAD	hot air drying
HID	hybrid hot air- infrared drying
FMCS	fuzzy-machine vision control System
A	area of slice (number of on pixels binary image)
Sh	shrinkage (%)
L^*	lightness value
a^*	redness value
b^*	yellowness value
ΔE	total color difference
T	air temperature (°K)
V	air velocity (m/s)
Q, W	energy (kW h)
E	total energy consumption (kW h)
X	length of control volume
Y	width of control volume
Z	height of control volume
I	radiation (W/cm^2)
MR	moisture ratio (dimensionless)
RH	relative humidity (dimensionless)
P	pressure (Pa)
C	specific heat (kJ/kg °C)
J	desirability value (dimensionless)
h	enthalpy (kJ/kg)
t	duration of drying (h)
ρ	density (kg/m^3)
ω	humidity ratio (kg/kg)

Subscripts

0	initial value
1	ambient conditions (outside dryer)
2	hot air conditions (inside dryer)
HA	hot air
Fan	fan
IR	infrared
a	air
da	dry air
ws	saturated vapor
wv	water vapor
at	atmospheric
we	vaporization

available in regard to using CVS for feedback control of drying process.

Therefore, the research objective was to develop general structure of intelligent control system for hybrid hot air-infrared dryer, using CVS for observation and fuzzy logic for decision making process. It was anticipated that FMCS permits real-time manipulation of process variables within optimal ranges, thereby minimizing the quality loss and energy consumption. To test this hypothesis, a laboratory-scale hybrid hot air- infrared dryer (HID) was constructed and used for kiwifruit drying. Multiple variables, such as moisture ratio (MR), energy (E), shrinkage (Sh) and total color change (ΔE) of kiwifruit slices dried at different temperatures and air velocities were monitored and analyzed in real time. Based on these preliminary experiments, a genetic algorithm was implemented in a Genetic Fuzzy System (GFS) framework with an adaptation and learning capability according to Herrera (2008). The GFS was employed to generate an optimized set of rules to be fed into the following fuzzy control system that was developed to optimize the drying effects. The performance of the control system was tested for kiwifruit drying, reflecting optimum levels of MR, E, SH and ΔE.

2. Materials and methods

2.1. Dryer

The constructed laboratory-scale hybrid hot air-infrared dryer was equipped with a CVS and a control system (Fig. 1). This dryer was used for both HAD and HID drying. The main parts of the hybrid dryer are: four IR lamps (250 W, SICCATHERM-RED, OSRAM, China), some electrical heating elements (total wattage of 7000 W), a fan (2000 m^3/h, equipped with a 0.75 kW three-phase electromotor, MOTOGEN, Iran), a digital weighing scale (±0.01 g, A&D Co., Japan) connected to a PC (for continuously measuring the sample's weight), an air duct, a wire meshed tray and three integrated temperature and relative humidity sensors, model AM2303, installed before and after the tray and the third one outside the dryer for measuring ambient air temperature and humidity. The distance between the IR lamps and the tray, determined from preliminary trials, was 20 cm. Also, the uniformity of IR radiation and temperature on the tray were confirmed by a thermal camera (NEC G120, Nippon Avionics Japan). Kiwifruit slices were placed on the tray over which the IR lamps were located. The whole body of the dryer was thermally insulated with fiberglass.

2.2. Computer Vision System (CVS)

The CVS consisted of a digital camera (COOLPIX P510, Nikon Co., Japan) and illumination chamber. The illumination chamber was composed of eight power LED lamps (5 W) placed 20 cm above the sample tray at the angle of 45° with respect to the sample plane (see #9 in Fig. 1) to provide uniform illumination. Computer hardware and software were developed to capture and process the 4608 × 3456 pixel images of the kiwifruit slices during drying. To capture the high quality images of the samples being dried without any influence from the ambient light exposure, the camera was placed outside of the drying chamber, but with its lens placed over an orifice facing directly downwards on the drying tray. A small, 12 V fan was installed adjacent to the camera for cooling. The captured images were transferred to a computer through a Wi-Fi memory card (model Eyefi Mobi, Eyefi Co., US). The captured images were, then, read and analyzed by MATLAB software (Mathworks Inc, US).

2.3. Image features extraction

Image processing was performed through an algorithm written in MATLAB. Image segmentation was among the pre-processing steps applied on the images. In these images, as the objects of interest, i.e. slices of kiwifruit, had a bright green color and the background (the tray) was black, a quality segmentation was obtained by Otsu's method based thresholding of the high contrast image of green and blue difference (2G-2B) (Otsu, 1975). After binarizing images, a morphological flood-fill operation was performed to fill the holes inside the regions of kiwi slices particularly due to the small black seeds. Several features including the area of slices and their color values were extracted from the pre and

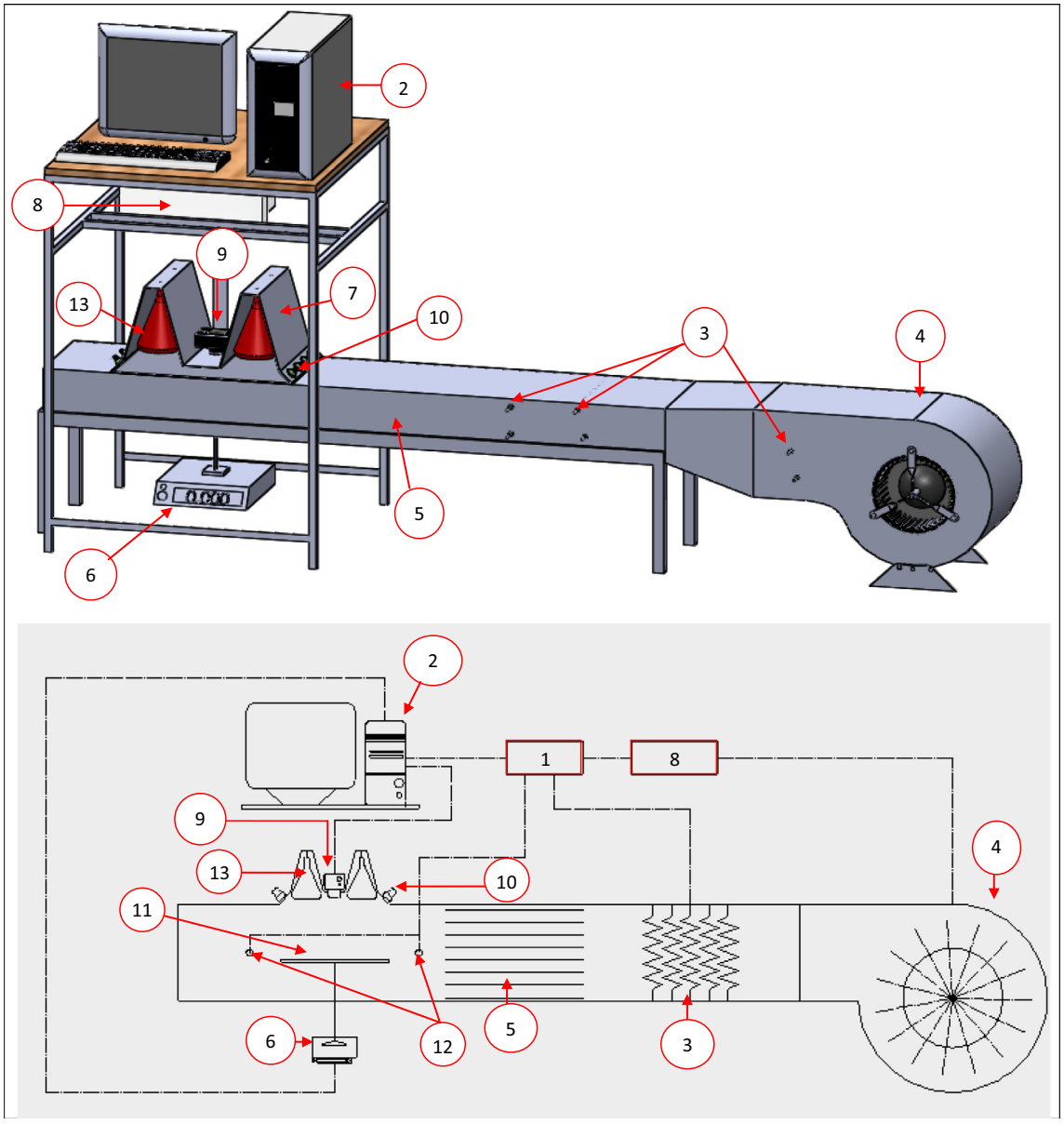

Fig. 1. Experimental dryer: (1) Control units; (2) PC; (3) Heating unit; (4) Fan; (5) Straightener; (6) balance; (7) Illumination and imaging chamber (a cutaway of chamber is displayed); (8) Inverter; (9) Camera; (10) Lighting lamp; (11) Tray; (12) Temperature sensors; (13) IR lamps (Nadian et al., 2016a).

post-processed images. The area of slice (A) was calculated by pixel count method and then the area shrinkage was defined as:

$$\text{Sh}\ \ (\%) = \frac{A_0 - A}{A_0} \times 100\% \tag{1}$$

where A_0 and A are the initial and current areas of slice, respectively.

Color changes during drying were determined by extracting the RGB color information from the kiwifruit pixels in the segmented images, and then were converted to L*a*b* color space. To standardize the extracted L*a*b* from the images, a regression model was used between Hunter Lab L*a*b* values and their corresponding CVS values of 20 standard colored papers in two conditions: when IR lamps were on and with no IR exposure (Nadian et al., 2015). The color values were averaged and used to calculate the total amount of color changes during fruit drying by Eq. (2) (Hosseinpour et al., 2013):

$$\Delta E = \sqrt{(L^* - L_0^*)^2 + (a^* - a_0^*)^2 + (b^* - b_0^*)^2} \tag{2}$$

where the values of L_0^*, a_0^* and b_0^* are the values of the lightness, the values of "green to red" and "yellow to blue" of a fresh sample, respectively.

2.4. Energy consumption

As seen in Fig. 2, the energy consumption (kW h) of the hybrid hot air-infrared dryer is the total energy in the control volume (Eq. (3)). This amount was calculated as the sum of the energy from hot air convection (Q_{HA}) and fan (W_{Fan}) plus the amount of energy emitted by IR lamps (Q_{IR}):

$$E = (Q_{HA} + W_{Fan} + Q_{IR}) \tag{3}$$

where:

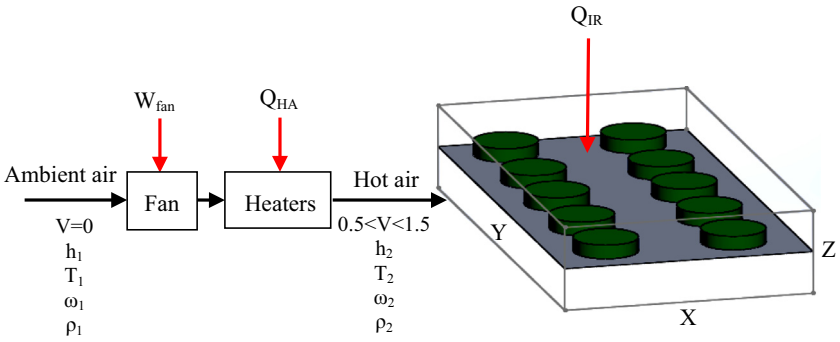

Fig. 2. Total energy flow into the control volume.

$$Q_{HA} + W_{Fan} = \rho_2 YZV[(h_2 - h_1) + (V^2/2000)]t/10^4 \quad (4)$$

$$Q_{IR} = I_{IR}\ XYt/10^3 \quad (5)$$

where X, Y and Z are the geometric dimensions of the control volume, which in this research were 10, 20 and 3 cm, respectively. The control volume was limited by the thickness of boundary layer, which was calculated in the assumption of laminar airflow, using Schmidt and Prandtl numbers (Asano, 2007; Fox et al., 2005). V is the air velocity inside the dryer (m/s); h_2 and h_1 are enthalpies of hot air and ambient air, respectively (kJ/kg); I_{IR} is the amount of infrared radiation received on the tray surface and was 0.3 W/cm^2 which is equal to the amount reported by others (Motevali et al., 2011; Ponkham et al., 2012; Supmoon and Noomhorm, 2013); t is the duration of drying (s) and ρ_2 is hot air density (kg/m^3). Air density varies with temperature, relative humidity and atmospheric pressure. Air density can be calculated through Eqs. (6)–(11) (Gebreegziabher et al., 2014; Jones, 2007):

$$\rho_a = \rho_{da}(1 + \omega)/(1 + 1.609\omega) \quad (6)$$

$$\omega = \frac{0.62198RH}{\frac{P}{P_{ws}} - RH} \quad (7)$$

$$P_{ws} = \frac{\exp\left(77.3450 + 0.0057T - \frac{7235}{T}\right)}{T^{8.2}} \quad (8)$$

$$\rho_{da} = 0.0035\ P_{da}/T \quad (9)$$

$$P_{da} = P_{at} - P_V \quad (10)$$

$$P_V = RH \times P_{ws} \quad (11)$$

where ρ_a is air density (kg/m^3); ρ_{da} is dry air density (kg/m^3); ω is humidity ratio and expressed as water vapor mass per dry air mass (kg/kg); RH is relative humidity; P_{ws} is saturation pressure of water vapor (Pa); T is dry bulb temperature, usually referred to as air temperature (K); P_{da} is the partial pressure of air (Pa); P_v is the partial pressure of water vapor in moist air (Pa) and P is the atmospheric pressure of moist air in the testing location (Pa).

The enthalpy changes of air $(h_2 - h_1)$ is calculated using Eq. (12) (Akpinar, 2004; Kutz, 2015):

$$h_2 - h_1 = C_a(T_2 - T_1) + C_V(\omega_2 T_2 - \omega_1 T_1) + h_{we}(\omega_2 - \omega_1) \quad (12)$$

where the subscripts 1 and 2 refer to ambient and hot air, respectively. C_{pa} is the specific heat capacity of air at constant pressure. C_a can be set to 1.006 kJ/kg °C for an air temperature between −100 °C and 100 °C. C_V is the specific heat of water vapor at constant pressure (1.84 kJ/kg °C) and h_{we} is the specific heat of water evaporation at 0 °C (2502 kJ/kg).

2.5. Experimental procedure

The kiwifruits (*Actinidia deliciosa cv Hayward*) were cold stored at 5 °C before any experiment for a seven day period in order to slow down the respiration, physiological and chemical changes. The initial moisture content of kiwifruits was 82 ± 1% wet basis (w.b.), according to the vacuum oven method at 105 °C for 12 h (Nadian et al., 2015). Just before experiment kiwifruits were cut into slices perpendicular to the fruit axis with a uniform thickness of 3 mm using a fixed coping saw after washing and peeling. The dimensionless refractive index of the samples was determined as 13.95 ± 0.25, showing that the fruit samples were of the same ripening condition. To prevent enzymatic browning during the initial stage of drying, kiwifruit slices were pre-treated by hot water blanching (75 °C) for 5 min (Nadian et al., 2016b). The pre-treated slices were placed on the dryer's tray after the dryer reached a steady-state condition. Drying experiments were conducted at air temperatures of 50, 60, and 70 °C; air velocities of 0.5, 1 and 1.5 m/s and slice thickness of 3 mm. During drying experiments, top view images, temperature and relative humidity of ambient air, inlet and outlet air, and sample weight loss were recorded at 30 s intervals. Each drying experiment stopped when the samples' moisture ratio reached to 0.05.

2.6. Artificial neural network (ANN) development

Two ANNs (ANN-1 and ANN-2) were employed. The former was in charge of optimizing the fuzzy controller using Genetic Algorithm and the latter was responsible for predicting the MR of materials being dried based on image information (ΔE and Sh). These networks were designed based on some preliminary drying experiments with HID and HAD modes and various temperatures (50, 60, and 70 °C), air velocities (0.5, 1 and 1.5 m/s) and three replications, producing 6302 data patterns considering the recording rate at 30 s interval (Nadian et al., 2016a). The data was randomized and divided into three categories for training (60%), validation (15%), and testing (25%) (Nadian et al., 2015). The ANN-1 network was used to predict the kiwifruit drying characteristics including ΔE, Sh and MR with four input variables: time, IR lamps mode (ON = 1 and OFF = 0), temperature (T) and air velocity (V). The ANN-2 network was employed for predicting sample's MR from ΔE and Sh as inputs. Training of ANN-2 was provided separately on two sets of data for HID and HAD. In order to design these networks, different ANN configurations with a supervised multi-

layered perceptron (MLP) trained by back propagation (BP) algorithm was developed by modifying both the number of neurons (1–20) and the number of hidden layers (1–2) using MATLAB coding. Two statistical parameters including the coefficient of determination (R^2) and mean square error (MSE) were used to evaluate the goodness of fit for the selected topologies. It is worth pointing out that all data sets except IR lamps mode before ANN configuration were normalized between (−0.9 and 0.9) using the min-max function as follows (Nadian et al., 2015):

$$Y_{normalized} = -0.9 + 1.8\frac{Y_i - Y_{min}}{Y_{max} - Y_{min}} \quad (13)$$

2.7. Designing fuzzy control system using genetic algorithm

To optimize the dryer control and to perform a drying process with the shortest drying time and the highest quality of dried fruit, a fuzzy controller was developed. The output of the intelligent control system was a new series of set-points (air velocity, IR lamps mode and temperature) affecting the drying process. A sub-control unit was used to manipulate these variables, which are read by sensors, to match as close as possible to the values of the set points by reducing errors. This sub-control unit interfaced to a computer through a RS-232 port. A microcontroller (ATmega16) was employed to process the sensors' data (temperature, relative humidity and air velocity). The controller was programmed using MATLAB v7 (Mathworks Inc, US) to execute several tasks such as reading measurements and manipulating suitable control signals for the fan, the IR lamps and the heater elements. The airflow velocity was adjusted by changing the rotational speed of the fan via an inverter (model Hyundai N50, US). The IR lamps were controlled in an ON/OFF mode.

To regulate the temperature, the required energy of the heater elements was controlled by adjusting ON/OFF duty cycle with pulse width modulation (PWM). The PWM technique allows controlling the heaters with various output levels and hence providing a smoother control of drying temperature (Javanmard et al., 2009). In our case the pulse width was adjusted employing a PID controller.

In the Fuzzy logic controller, three parameters (MR, Sh and ΔE) were chosen as input variables and the output variables were temperature (T), air velocity (V) and IR mode (ON/OFF). The inputs and outputs were ranged as: (0 < MR < 1); (0 < Sh < 25); (0 < ΔE < 15); (50 < T < 70); (0.5 < V < 1.5). These ranges were obtained based on the preliminary drying experiments. Three Gaussian membership functions (MFs) of low, medium and high were defined for the input and output variables (except for IR) by MATLAB Fuzzy Logic Toolbox. The IR values were defined as two Gaussian MFs of ON and OFF with the output rounded to integer constant (ON = 1 and OFF = 0). These functions were selected based on the fact that the Gaussian functions facilitate obtaining smooth, continuously differentiable hyper-surfaces of a fuzzy model (Piegat, 2013). Therefore, considering the number of possible combinations of input sets, including MFs of MR, Sh and ΔE, each having three levels (low, medium and high) plus a "none" status, the number of rules results in 64. Since "all-none" is not a valid input set, the number of rules becomes 64 − 1 = 63.

The fuzzy controller was incorporated in the dryer to provide faster drying rate, while preserving the quality of the dried fruits with less shrinkage and color changes, and minimizing the energy consumption. Therefore, a desirability function (J) was defined with respect to the same weight of dependent variables:

$$J = \left[\left(\frac{E_{MR\cong 0.05}}{\max(E)}\right) + \left(\frac{\Delta E_{MR\cong 0.05}}{\max(\Delta E)}\right) + \left(\frac{Sh_{MR\cong 0.05}}{\max(Sh)}\right) + \left(\frac{t_{MR\cong 0.05}}{\max(t)}\right)\right] \Big/ 4 \quad (14)$$

where "max" refers to the maximum values of E, ΔE, Sh and t (they were approximately 1 kW h, 15, 25% and 130 min, respectively) obtained from the preliminary experiments after each sample reached equilibrium MR (0.05). This method normalizes the variables of the "J" function to obtain comparable values with the same weight by assuming the minimum value of these variables is zero. The objective of fuzzy control was to minimize the desirability function. Hence, a suitable genetic coding was required to evaluate the value of "J" using the fuzzy system parameterization. Finding an appropriate fuzzy control system is equivalent to finding the parameters of output MFs that gives the optimum J. In this study, among different GFS methods, we used *Pittsburgh* approach, in

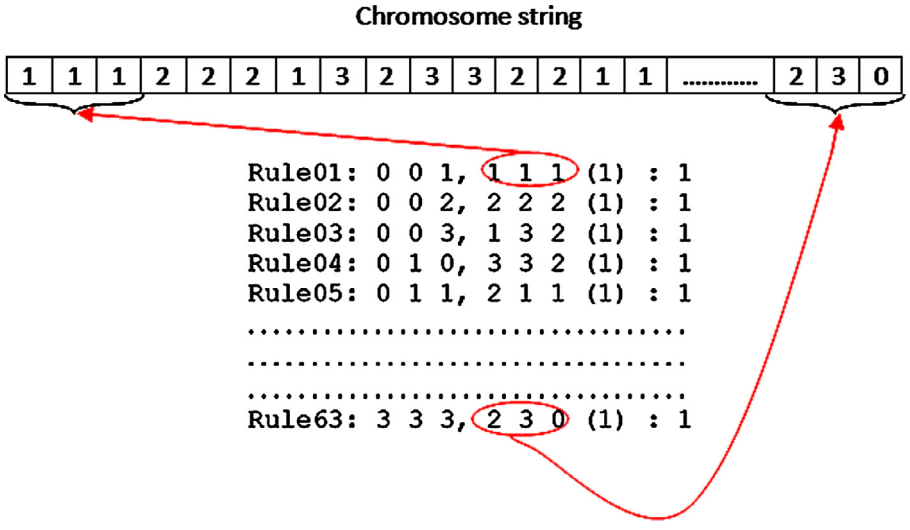

Fig. 3. Pittsburgh approach: a chromosome evolves a complete rule base.

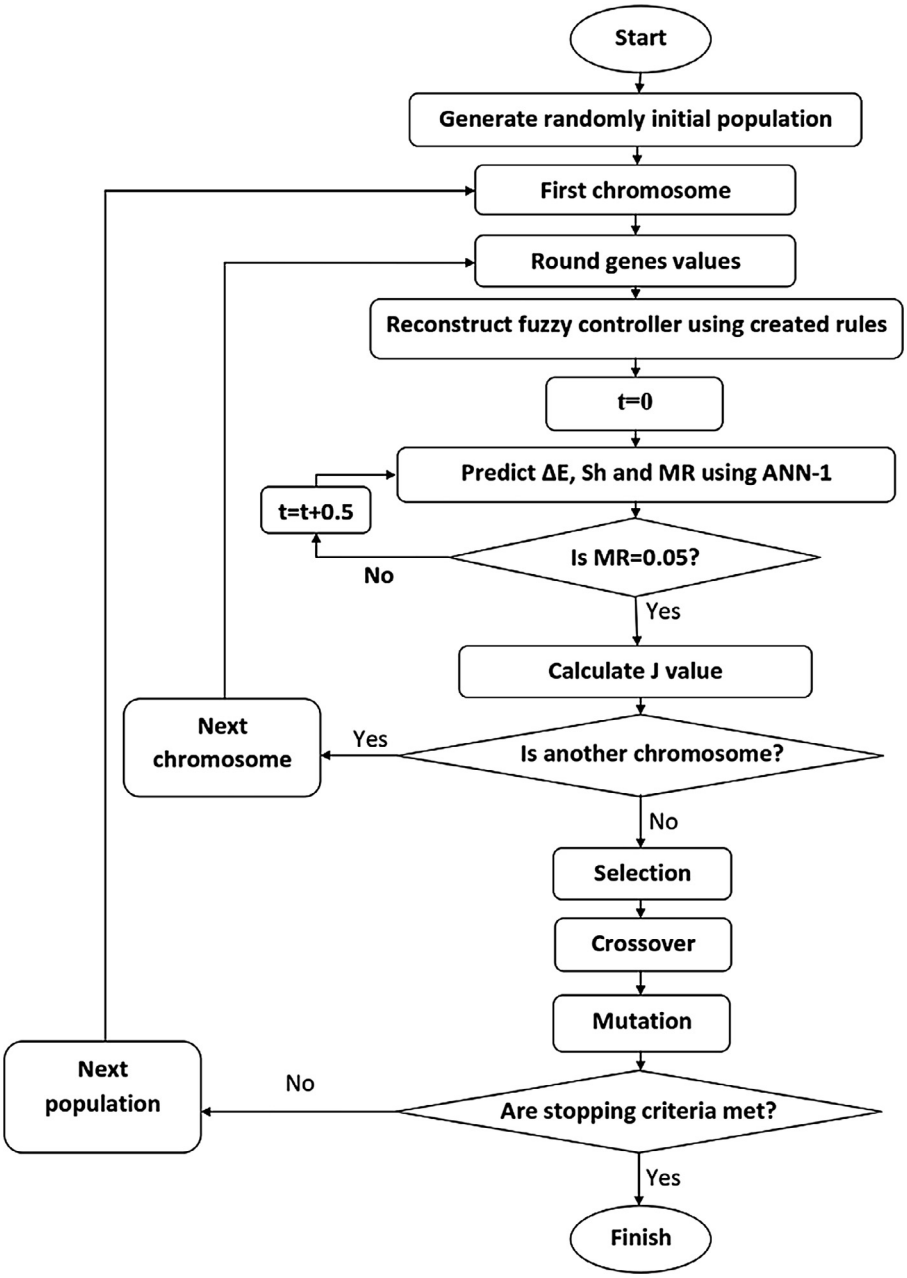

Fig. 4. The flowchart of GA optimization procedure.

which chromosomes represent a rule set (Herrera, 2008). In this approach each chromosome evolves in a complete rule base (Fig. 3). The overall procedure for optimization of fuzzy rule base using GA, illustrated in Fig. 4, includes the following steps:

1. The initial generation is random in the specified range (the values of chromosome are in the range of 0–3 for T and V; and 0–2 for IR mode (ON/OFF).
2. The elements of 189-demensional rounded string (chromosome) are distributed within 63 rules of 3 variables, V, T, IR (see Fig. 3). For instance, for the first rule, the first, second and third elements of the string form the first, second and third outputs of the first rule; corresponding to V, T and IR, respectively. The outputs of the next rules are formed from the next three-element sets of the string.
3. The output values of ANN-1 are calculated with a time interval of 0.5 min until equilibrium MR of 0.05 is reached (see Fig. 5).
4. The values of J are calculated for the GA population (population size = 200).
5. Forming a gene pool: recombination and mutation.
6. This procedure continues until either of stopping criteria (Generations = 100; Function tolerance = 10^{-6}; Nonlinear constraint tolerance = 10^{-6}) is reached.

2.8. Implementation and evaluation of the designed fuzzy control system

The optimal fuzzy control system obtained from GA was assessed using a hybrid hot air- infrared dryer under laboratory conditions. As shown in Fig. 6, the control unit was designed in

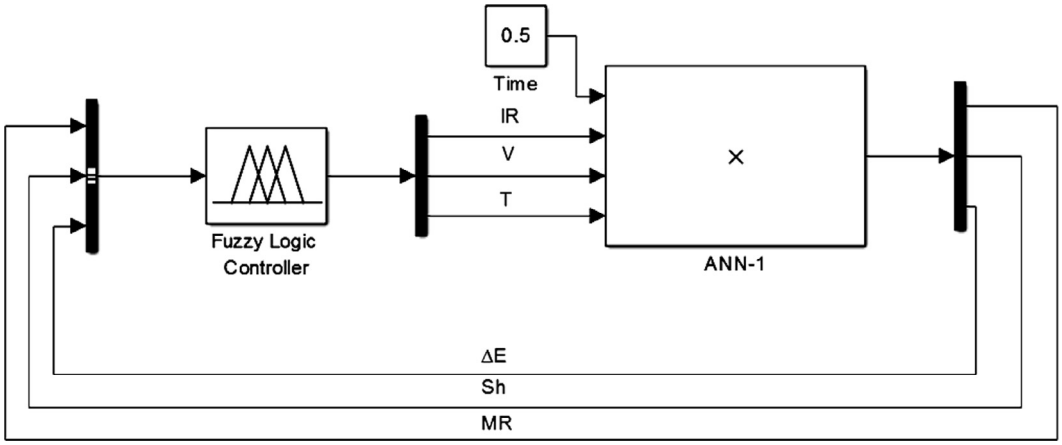

Fig. 5. Incorporating ANN-1 network to predict drying characteristics (ΔE, Sh and MR) for a single chromosome in the core section of the GA code to reach the final MR (0.05).

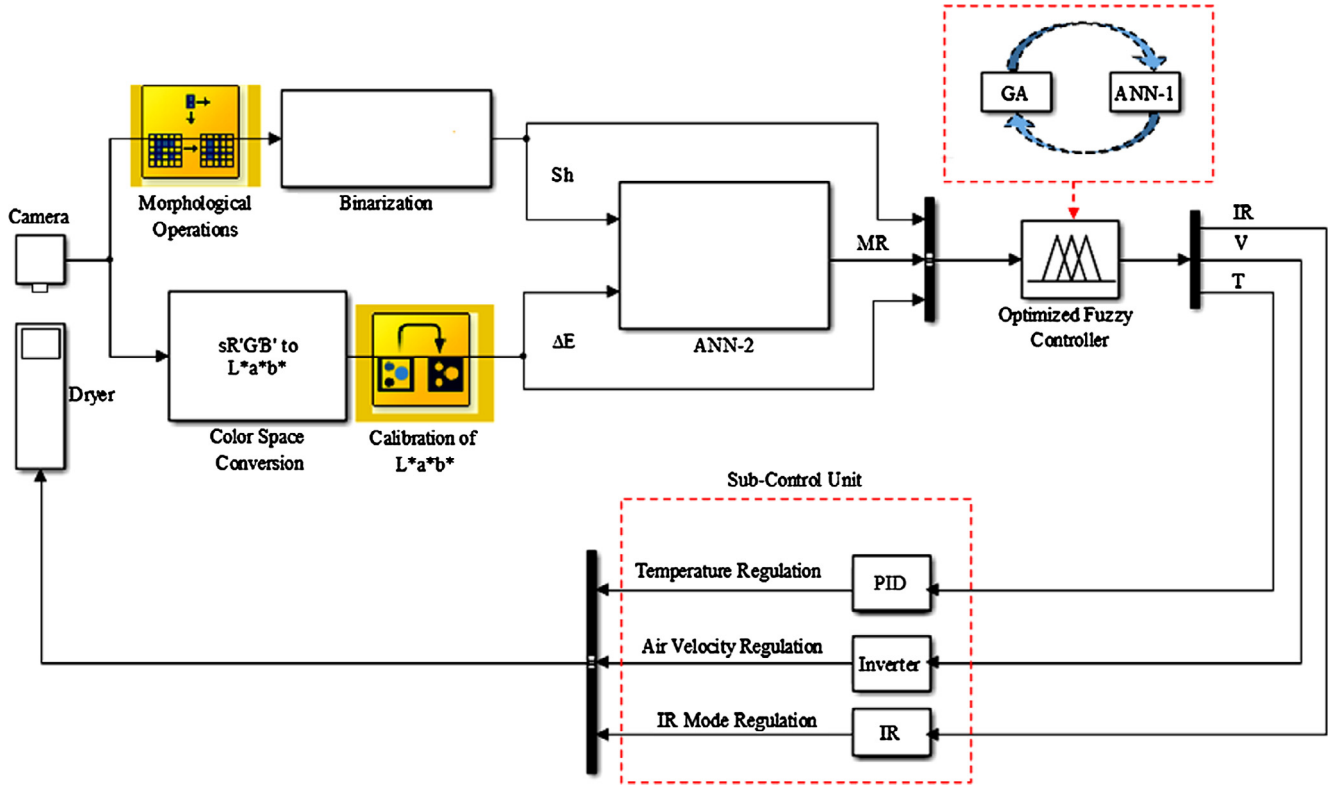

Fig. 6. The schematic diagram of the integrated control system.

such a way that requires only the image information (Sh and ΔE) as inputs. The MR values were predicted using ANN-2. The algorithm included several steps in the sequence:

1. Reading captured images at 3-min intervals (based on the dynamics of the drying system) to quantify the surface area of slices and their color values.
2. Predicting the MR for sample batch based on their Sh and ΔE using ANN-2.
3. Determining the optimized values of T, V and IR mode (ON or OFF) by the fuzzy control system.
4. Switching off the dryer when the MR reaches 0.05, otherwise going back to step 1.

To evaluate the performance of the developed fuzzy control, the values of J for kiwifruit slices were compared with the corresponding values obtained from drying experiments with no fuzzy control, i.e. HID and HAD conditions.

3. Results and discussion

3.1. ANN modeling

The structure of ANNs, containing two hidden layers with tangent sigmoid transfer functions, was trained by Levenberg–Marquardt learning algorithm. The topology of 4-5-13-3 for ANN-1

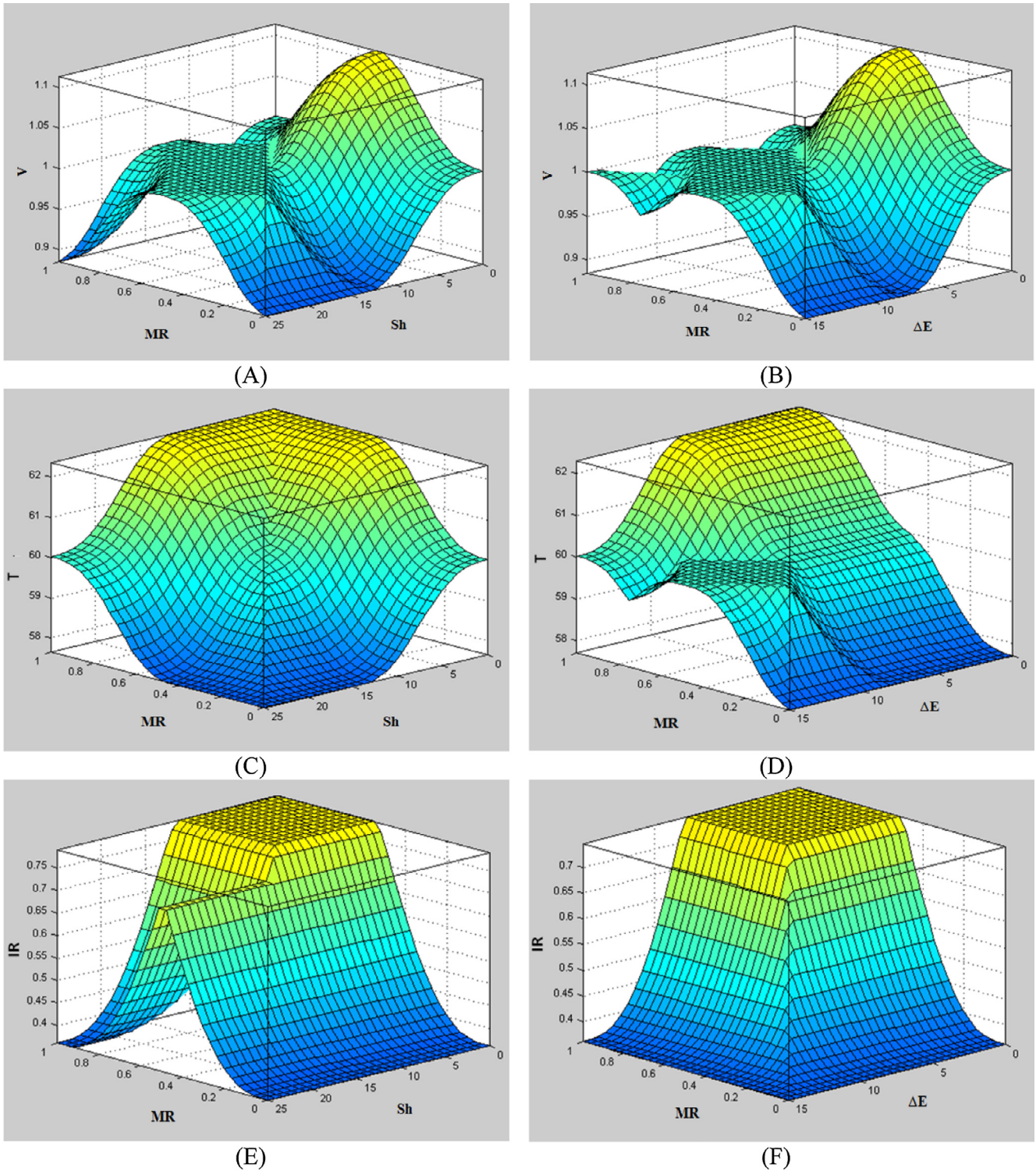

Fig. 7. Results of output surface of optimal FIS based on two inputs versus one output: (A) MR and Sh (%) vs. V (m/s); (B) MR and ΔE vs. V (m/s); (C) MR and Sh (%) vs. T (°C); (D) MR and ΔE vs. T (°C); (E) MR and Sh (%) vs. IR mode; (F) MR and ΔE vs. IR mode .

(R^2 = 0.9998 and MSE = 3.5×10^{-5}) and the topology of 2-8-11-1 for ANN-2 (R^2 = 0.9814 and MSE = 8.5×10^{-4}) were found to be the best suited due to their highest R^2 and lowest MSE.

3.2. Optimal fuzzy control

Fig. 7 shows the results of the output surface from an optimal fuzzy inference system (FIS) based on two inputs and one output from GFS. It is seen from this figure that the optimal range of V and T vary from 0.85 to 1.15 m/s and from 57.5 to 62.5 °C, respectively. Also it is worth pointing out that IR values must be rounded so that if the fractional part is less than 0.5, the IR lamps are OFF, otherwise, they are ON. This fuzzy controller was linked to the previously developed machine vision system to make an optimal FMCS. The laboratory dryer was controlled by the FMCS system and operated under laboratory conditions. According to the FIS

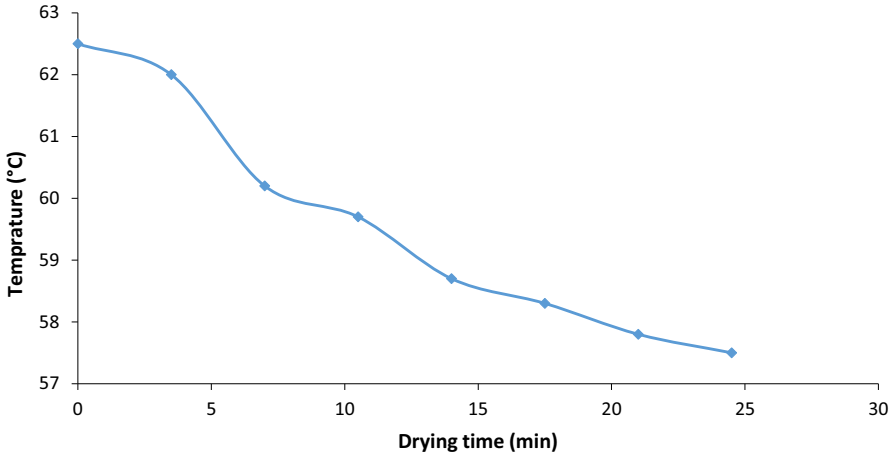

(A)

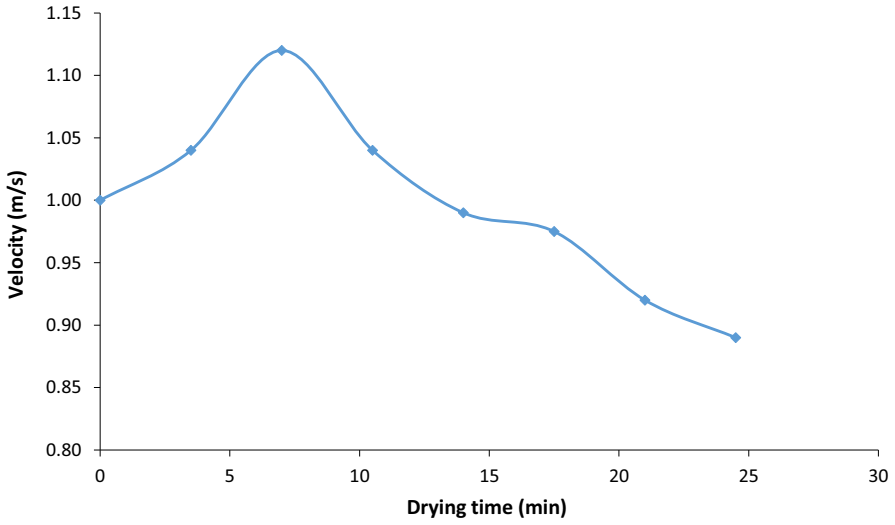

(B)

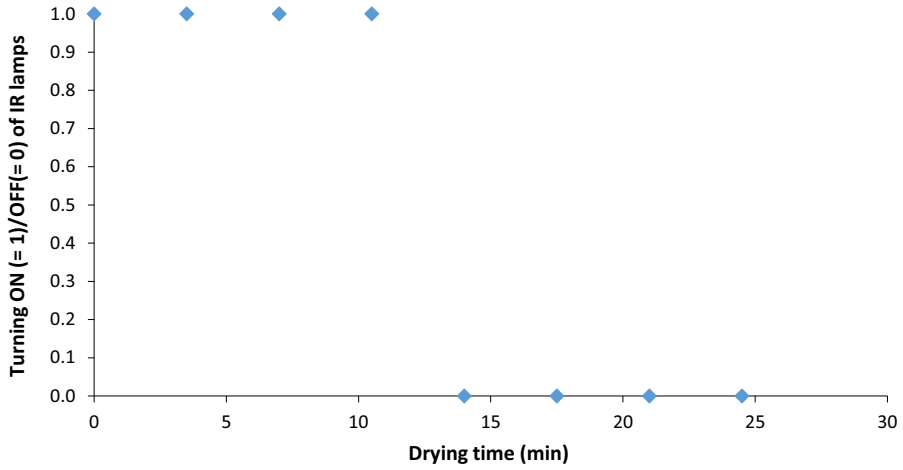

(C)

Fig. 8. Evolutions of velocity, temperature and IR mode versus drying time, during testing of FMCS.

Table 1
The lowest "J" values for HAD and HID drying methods in comparison with the value from FMCS.

Drying method	J
HAD (70 °C - 1.5 m/s – 3 mm)	0.4345
HID (70 °C - 0.5 m/s – 3 mm)	0.3429
FMCS	0.2701

surfaces, the initial values for T, V and IR mode at the start of drying operations, when Sh and ΔE were zero and MR was 1, were 62.5 °C, 1 m/s and "ON", respectively. Three minutes later the new values of T, V and IR mode were determined from the image-extracted ΔE and Sh of kiwifruit slices. The evolutions of V, T and IR mode versus drying time during the testing fuzzy control system are shown in Fig. 8. The results suggest that drying should be carried out in a two-stage process: first HID and then HAD (see Fig. 8C). Moreover, the drying temperature should be started at its maximum possible value and then gradually decreased to prevent product overheating and the consequent browning /burning of the product and other deteriorations of the product (see Fig. 8A). As seen in Fig. 8B, the air velocity should be started at its moderate value gradually increasing to its maximum value (1.12 m/s) at the end of the first stage of the process with the next decreasing at the second stage to its minimum value (0.89 m/s). The air velocity controls the slices' temperature variations during the HID stage. Indeed, according to Nowak and Lewicki (2004), the excessive air velocity reduces the slices' surface temperature during HID process. Therefore, a short period after commencing the drying process, the temperature dropped as the air velocity increased to prevent overheating. Then, the hot air velocity gradually decreased to reduce the slices surface temperature with a smooth trend (see Fig. 8B). The knowledge derived from these results is that the correlation between temperature and air velocity should be negative at the first stage of drying and positive at the second stage of drying.

3.3. Evolutions of color change (ΔE), shrinkage (Sh) and energy consumption (E)

The lowest values of "J" (Eq. (14)), among all HID and HAD drying experiments, were observed from the treatments having air temperature of 70 °C and velocity of 0.5 m/s in HID conditions; and air temperature of 70 °C and velocity of 1.5 m/s in HAD conditions. Therefore, these treatments were selected as the best conditions for HID and HAD drying of kiwifruit. The values of "J" for these two methods and also for the designed FMCS are shown in Table 1. Also, drying curves (MR vs. Drying time) and the trends of ΔE, Sh and E changes as functions of MR are presented in Fig. 9. Generally, the IR exposure was the key factor, affecting the drying trend (Fig. 9A). The moisture of HID samples evaporated faster than HAD samples. This is because the thermal energy in HID drying is directly applied to the samples and it creates a large gradient of vapor pressure between the interior and the surface of the products. Although the HID considerably reduced the drying time, it did not meet expectations for product quality. As can be seen, HID drying resulted in higher shrinkage (Fig. 9B) and more color deterioration (Fig. 9C). It could be explained that at the higher temperature of IR exposure, the difference between the temperature of the samples and the glass transition temperature were higher and therefore the matrix mobility was not sufficient to support the structure of the solid material and hence collapse took place (Champion et al., 2000). Negligible difference in the shrinkage between HAD, HID and FMCS indicates that fuzzy control strategy did not affect internal microstructure of the material under drying. Regarding color changes, the results showed a general trend of discoloration with the decrease of moisture content (Fig. 9C). However, the increasing trend of ΔE was steeper for samples under HID drying than those under HAD conditions. The general increase of ΔE during the drying process can be explained by Maillard reaction by which the interactions between sugars and amino acids at high temperature lead to the formation of brown compounds. Therefore, the absorption of IR heat by drying material was probably the main reason for the higher ΔE in HID dried samples. This seemed to be due to the increase of the non-enzymatic browning rate especially at the final stage of drying, when the temperature was the highest and the moisture content reached its minimum. In this regard, Garza et al. (1999) indicated a clear dependency between non-enzymatic browning rate and temperature.

In terms of energy consumption, the results showed that HAD drying consumed more energy in control volume than under HID conditions (Fig. 9D). The energy consumption in control volume for HID method was 0.108 kW h as compared to 0.530 kW h for HAD. In other words, the energy consumption of HAD method was nearly five times higher than the HID method, indicating much higher energy efficiency of HID. Despite the shorter drying time and less energy consumption of HID drying method, it did not provide the best quality in terms of color and shrinkage. Hence, a possible solution for improving the quality of the end product could be accomplished with an automated manipulation of drying variables. FMCS energy consumption was 0.158 kW h, which is a little bit higher than HID, however it is significantly less than HAD strategy. This increase of energy consumption in FMCS compared to HID is the ultimate cost for the quality preservation, because introducing HAD at the second stage would require four minutes longer drying.

From Fig. 9 it follows that HAD can preserve quality; however it is longer and, therefore, more energy consuming. On the other hand, HID facilitates drying and, therefore, saves energy; however damaging for quality in certain periods of drying. Results indicate that introducing of HID at the beginning of the drying process does not create too much harm to the color. As seen in Fig. 9, the FMCS, which is a combination of the HID and HAD methods with an automatic control of drying variables, represents a good balance between the energy consumption and the quality of dried kiwifruits. It was found that developed FMCS could decrease the drying time and energy consumption effectively (compared to HAD) and with little color changes (compared to HID). The minimal difference between FMCS and HAD in color along with the minimal difference between FMCS and HID in energy consumption satisfies objective of the control. Also, as shown in Table 1, the J value of FMCS in comparison with the best condition of HID and HAD methods confirmed that a real time vision-system monitoring in conjunction with a fuzzy controller could optimize both the energy consumption and product quality.

One could assume that the performance of HID could be improved simply by turning ON IR lamps only for the first 15 min and then turning them OFF. However, it should be noted that this simplification is possible only for the particular case of kiwifruit drying in specified range of temperatures and velocities; however it could not be generalized for other drying applications. On the other hand, developed general structure of intelligent (fuzzy) control system is applicable for any material and operating conditions.

4. Conclusions

In this study, a FMCS was developed for a real time control of thin layer kiwifruit slices drying in a hybrid hot air-infrared dryer. The Genetic Algorithm was employed to optimize the fuzzy controller. The resulting Genetic Fuzzy System (GFS) was then used

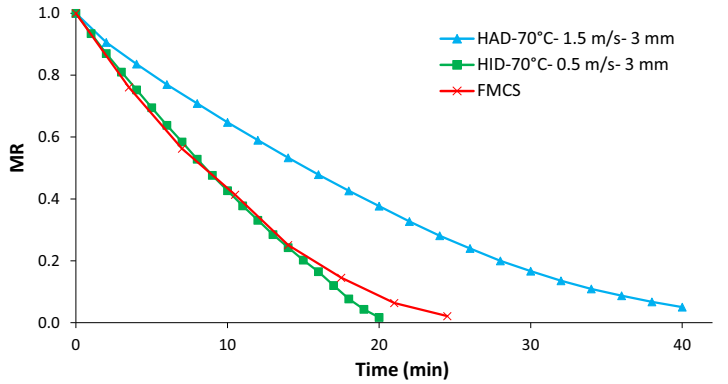

(A)

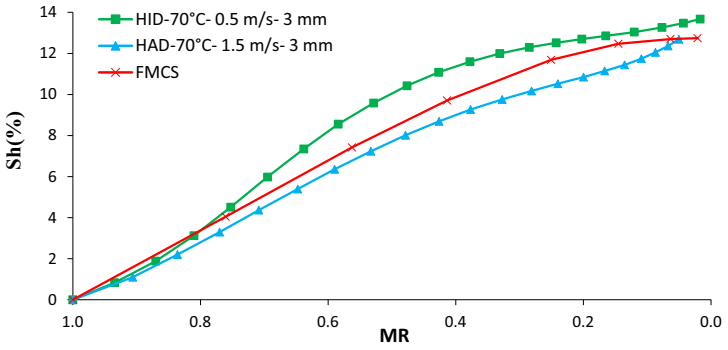

(B)

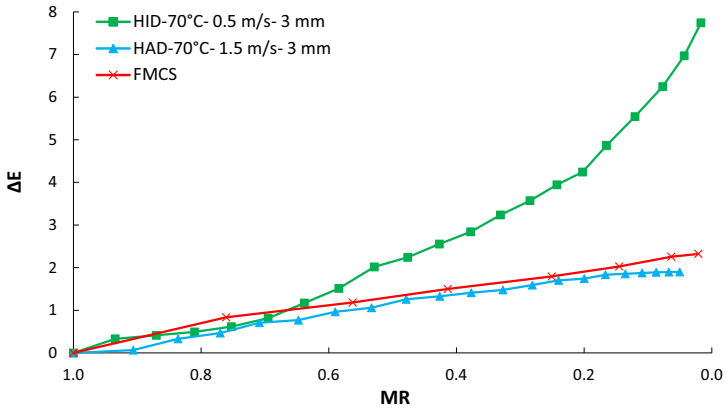

(C)

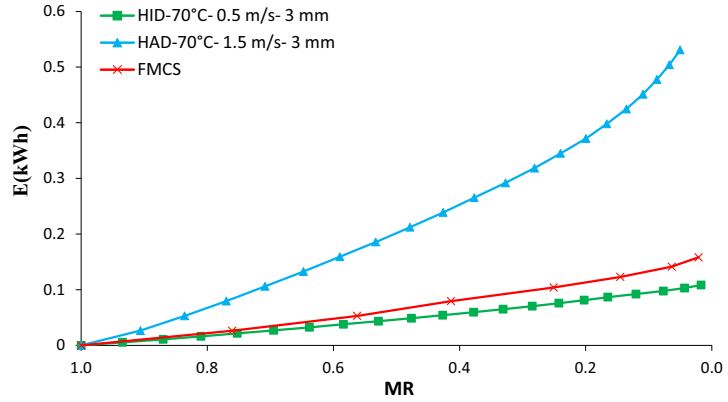

(D)

Fig. 9. Relationships between MR and drying time (A); Sh and MR (B); ΔE (color change) and MR (C); and E (Energy consumption) and MR (D) for optimal condition of HID and HAD drying methods as well as FMCS of drying.

for optimization of drying variables. The results showed that the HID drying method considerably reduced the drying time compared with HAD method, but it could not provide the best quality product in terms of color changes and shrinkage. FMCS reduces the drying time compared to sole HAD drying from 40 to 24 min (40%) and improve quality as compare to sole HID drying in terms of color changes ΔE from 7.9 to 2.1 (more than three times). Therefore, the FMCS can be employed for automatic in-line control of foodstuffs quality in various drying operations.

Acknowledgment

The authors acknowledge and appreciate the funding support provided by the Ferdowsi University of Mashhad – Iran for this project.

References

Akpinar, E.K., 2004. Energy and exergy analyses of drying of red pepper slices in a convective type dryer. Int. Commun. Heat Mass Transfer 31, 1165–1176.
Asano, K., 2007. Mass Transfer: From Fundamentals to Modern Industrial Applications. Wiley.
Campos-Mendiola, R., Hernández-Sánchez, H., Chanona-Pérez, J., Alamilla-Beltrán, L., Jiménez-Aparicio, A., Fito, P., Gutiérrez-López, G., 2007. Non-isotropic shrinkage and interfaces during convective drying of potato slabs within the frame of the systematic approach to food engineering systems (SAFES) methodology. J. Food Eng. 83, 285–292.
Champion, D., Le Meste, M., Simatos, D., 2000. Towards an improved understanding of glass transition and relaxations in foods: molecular mobility in the glass transition range. Trends Food Sci. Technol. 11, 41–55.
Chen, Y., Martynenko, A., 2013. Computer vision for real-time measurements of shrinkage and color changes in blueberry convective drying. Drying Technol. 31, 1114–1123.
Fox, R.W., McDonald, A.T., Pritchard, P.J., 2005. Introduction to Fluid Mechanics. Wiley.
Garza, S., Ibarz, A., Pagán, J., Giner, J., 1999. Non-enzymatic browning in peach puree during heating. Food Res. Int. 32, 335–343.
Gebreegziabher, T., Oyedun, A.O., Luk, H.T., Lam, T.Y.G., Zhang, Y., Hui, C.W., 2014. Design and optimization of biomass power plant. Chem. Eng. Res. Des. 92, 1412–1427.
Hebbar, H.U., Vishwanathan, K., Ramesh, M., 2004. Development of combined infrared and hot air dryer for vegetables. J. Food Eng. 65, 557–563.
Herrera, F., 2008. Genetic fuzzy systems: taxonomy, current research trends and prospects. Evol. Intel. 1, 27–46.
Herrera, F., Lozano, M., Verdegay, J.L., 1998. A learning process for fuzzy control rules using genetic algorithms. Fuzzy Sets Syst. 100, 143–158.
Hosseinpour, S., Rafiee, S., Mohtasebi, S.S., 2011. Application of image processing to analyze shrinkage and shape changes of shrimp batch during drying. Drying Technol. 29, 1416–1438.
Hosseinpour, S., Rafiee, S., Mohtasebi, S.S., Aghbashlo, M., 2013. Application of computer vision technique for on-line monitoring of shrimp color changes during drying. J. Food Eng. 115, 99–114.
Javanmard, M., Abbas, K., Arvin, F., 2009. A microcontroller-based monitoring system for batch tea dryer. J. Agric. Sci. 1, p101.
Jones, W.P., 2007. Air Conditioning Engineering. Taylor & Francis.
Kutz, M., 2015. Mechanical Engineers' Handbook. Wiley, Energy and Power.
Li, Z., Raghavan, G.V., Wang, N., 2010. Carrot volatiles monitoring and control in microwave drying. LWT-Food Sci. Technol. 43, 291–297.
Motevali, A., Minaei, S., Khoshtaghaza, M.H., Amirnejat, H., 2011. Comparison of energy consumption and specific energy requirements of different methods for drying mushroom slices. Energy 36, 6433–6441.
Mujumdar, A.S., 2014. Handbook of Industrial Drying. Taylor & Francis.
Nadian, M.H., Rafiee, S., Aghbashlo, M., Hosseinpour, S., Mohtasebi, S.S., 2015. Continuous real-time monitoring and neural network modeling of apple slices color changes during hot air drying. Food Bioprod. Process. 94, 263–274.
Nadian, M.H., Abbaspour-Fard, M.H., Sadrnia, H., Golzarian, M.R., Tabasizadeh, M., Martynenko, A., 2016a. Improvement of kiwfruit drying using computer vision system (CVS) and ALM clustering method. Drying Technol. (accepted)
Nadian, M.H., Abbaspour-Fard, M.H., Sadrnia, H., Golzarian, M.R., Tabasizadeh, M., 2016b. Optimal pretreatment determination of kiwifruit drying via online monitoring. J. Sci. Food Agric. 96, 4785–4796.
Nowak, D., Lewicki, P.P., 2004. Infrared drying of apple slices. Innovative Food Sci. Emerging Technol. 5, 353–360.
Otsu, N., 1975. A threshold selection method from gray-level histograms. Automatica 11, 23–27.
Piegat, A., 2013. Fuzzy modeling and control. Physica.
Ponkham, K., Meeso, N., Soponronnarit, S., Siriamornpun, S., 2012. Modeling of combined far-infrared radiation and air drying of a ring shaped-pineapple with/without shrinkage. Food Bioprod. Process. 90, 155–164.
Supmoon, N., Noomhorm, A., 2013. Influence of combined hot air impingement and infrared drying on drying kinetics and physical properties of potato chips. Drying Technol. 31, 24–31.
Yadollahinia, A., Jahangiri, M., 2009. Shrinkage of potato slice during drying. J. Food Eng. 94, 52–58.
Zhang, M., Jiang, H., Lim, R.-X., 2010. Recent developments in microwave-assisted drying of vegetables, fruits, and aquatic products—drying kinetics and quality considerations. Drying Technol. 28, 1307–1316.
Zhang, M., Tang, J., Mujumdar, A.S., Wang, S., 2006. Trends in microwave-related drying of fruits and vegetables. Trends Food Sci. Technol. 17, 524–534.